Presented at the Optical Society of America Conference on Soft X-Ray Projection Lithography, Monterey, California, April 1992

Conf-9204120--4
BNL-48033

Synchrotron Radiation Sources and Condensers for Projection X-Ray Lithography.*

J.B.Murphy
National Synchrotron Light Source, Brookhaven National Laboratory, Upton, NY 11973

D.L.White
AT&T Bell Laboratories, 600 Mountain Av., Murray Hill, NJ 07974

A.A.MacDowell
AT&T Bell Laboratories, 510E Brookhaven Laboratory, Upton, NY 11973

O.R.Wood II
AT&T Bell Laboratories, Crawfords Corner Road, Holmdel, NJ 07733

BNL--48033
DE93 002964

Abstract

The design requirements for a compact electron storage ring that could be used as a soft x-ray source for projection lithography are discussed. The design concepts of the x-ray optics that are required to collect and condition the radiation in divergence, uniformity and direction to properly illuminate the mask and the particular x-ray projection camera used are discussed. Preliminary designs for an entire soft x-ray projection lithography system using an electron storage ring as a soft X-ray source are presented. It is shown that by combining the existing technology of storage rings with large collection angle condensers, a powerful and reliable source of 130Å photons for production line projection x-ray lithography is possible.

PREPRINT
August 28, 1992
To appear in the Proceeding of the Optical Society of America Conference on Soft X-Ray Projection Lithography.

Received by OSTI
NOV 1 6 1992

MASTER

*This work was performed under the auspices of the U.S. Dept. of Energy.

DISTRIBUTION OF THIS DOCUMENT IS UNLIMITED

TECHNICAL MEMORANDUM

1. Introduction

Over the past two years various research teams (1,2,3) have demonstrated that Soft X-Ray Projection Lithography (SXPL) is a potential lithographic technique to print 0.1μm features that are considered a likely requirement for integrated circuits around the turn of the century. To date this lithography has been demonstrated to work using photons at a wavelength around 130Å. Possible sources of this soft X-ray radiation are laser plasma sources (4,5) and synchrotron radiation from electron storage rings (6). Plasma sources generated by pulsed laser light suffer from low output, low repetition rate and a debris problem. Such sources are presently under development to overcome these shortcomings. On the other hand electron storage rings are a well developed technology, do not have a debris problem and they are commercially available. Small storage rings have been built that have proved to be reliable and compact (7). This paper discusses the design requirements for a small compact storage ring that could be used as a soft x-ray source for SXPL. Also discussed are the design concepts of the x-ray optics that are required to collect the radiation and illuminate the mask in a manner that is matched to the particular SXPL camera used. Finally, preliminary designs for an entire SXPL system are presented.

2. Source Power Requirements

A previous analysis (8) indicated that the production print rate requirement would be of the order of about 1cm²/sec. This is equivalent to a print rate of about fifteen 6 inch wafers per hour. At present, resists have not been developed and optimized for exposure with light of wavelength equal to 130Å. The analysis (8) indicated that a sensitivity of about 5mJ/cm² was a likely requirement for the resist. A more sensitive resist of about 1mJ/cm² would suffer from shot noise effects that would make the edge walls ragged, whereas a resist of sensitivity of greater than ~10mJ/cm² would reduce throughput. Several designs of possible soft x-ray cameras have been presented in the literature (9,10). They consist of 2, 3 or 4 normal incidence aspheric mirrors. Such mirrors are required to be coated with alternate layers of Molybdenum and Silicon that can have a normal incidence reflectance of up to 61% at a wavelength of ~130Å (10). The raw power requirements of the source is given simply by

$$\text{Source Power} = \frac{\text{Power on Resist}}{(\text{Multilayer Reflectivity})^n \times \text{Collection Optics Efficiency}}$$

where n is the number of multilayer mirror reflections within the camera including a multilayer reflection mask (12).

It is anticipated that a SXPL printer would use resist of sensitivity of 5mJ/cm², a three

mirror projection camera and reflection mask with multilayer mirror reflectivity of 60% and a condenser system (that will be described later) with a throughput of ~30%. This defines the source requirements to be 128 mwatts of 130Å radiation.

At the present time there are significant uncertainties associated with the new multilayer technology and the as yet undeveloped resist technology. For instance, carbon contamination problems (13) can reduce multilayer mirror reflectivity, which in the drastic case of reducing multilayer reflectivity from 60% to 36% would require the source to output 1 watt of radiation. Such problems indicate that the source may be required to supply much more power than the 128 mwatts estimated above. It is prudent at this stage in the progress of SXPL, to design the source and collection optics to supply about an order of magnitude higher flux, say for example 1 watt of 130Å radiation. In the fortuitous event of still only requiring a source power of 128 mwatts, the additional power can readily be used to increase wafer throughput. Finally the bandpass requirements of the radiation are determined by the overlap of the bandpasses of the individual multilayer mirrors (14), which in the case of 4 or 5 multilayer mirrors is about 2.6% and 2.3% bandpass respectively. This raw power of 1 watt of 130Å radiation within a 2% bandwidth is the requirement of any x-ray source to be used by SXPL.

3. Electron Storage Ring Parameters

Electron storage rings consist of relativistic electrons circulating in vacuum in the horizontal plane. The electrons are confined by magnetic fields. When the electrons are bent round a radius by a magnetic field, the accelerated electrons emit synchrotron radiation in a radial fan that is well collimated in the vertical plane.

The synchrotron radiation power output at a given wavelength λ, in a bandwidth $\Delta\lambda/\lambda$, integrated over all vertical angles is given by (15) -

$$Power(\lambda)(mW) = 8.73 \times 10^3\, E^4\,(GeV)\, I(amp)\, \Theta(mrad)\, (\Delta\lambda/\lambda)\, G_2(y) \,/\, \rho(m)$$

where $y = \lambda_c/\lambda$ and $G_2(y)$ is given by,

$$G_2(y) = y^2 \int_y^\infty K_{5/3}(x)\,dx$$

and where $K_{5/3}(x)$ is a bessel function and λ_c is the critical wavelength given by

$$\lambda_c(\text{Å}) = 5.59\, \rho(m) \,/\, E^3(GeV).$$

Figure 1 shows the dipole radiation power output versus wavelength for three different electron energies of 400 MeV, 600 MeV and 800 MeV with a bending magnet field of 1.4 Tesla. The figure shows that increasing the electron energy results in only a slightly higher power at 130Å. For instance increasing the electron energy from 600MeV to 800MeV only

results in a 20% increase of the flux available at 130Å with most of the increased power output producing hard x-rays below 50Å. The cost and size of the ring scale with the electron energy, so low energy rings are the more favored. The electron energy can only be reduced so much before coulomb scattering of the electrons start to significantly diminish the lifetime of the stored beam. The overall size of the ring is dependant on the field of the dipole magnets - the higher the magnetic field the smaller the ring. A value of 1.4 Tesla represents a high but achievable field for conventional electromagnets. Superconducting magnets have not been considered in this paper from a cost, complexity and reliability viewpoint.

The curve for 600MeV electrons in figure 1 is a reasonable compromise between the various conflicting requirements. Such a 600MeV ring has an output at 130Å of 1.0 watt/500mA/0.5 rad(horizontal)/all vertical angles/2% bandpass. To achieve the 1.0 watt power requirement at 130Å, a total of 500 mrads are thus required to be collected with the storage ring operating at 500mA. This represents the typical horizontal collection angle that an illuminator system should collect from a low energy storage ring. 2π radians of horizontal radiation are available for collection, so a storage ring could in principle be a source for up to 12 lithography cameras.

4. Storage Ring Design

A suitable lattice for a small 600MeV storage ring would be the two superperiod Double Bend Achromat lattice consisting of four combined function dipole magnets and six combination quadrupole/sextupole magnets. Figure 2 is a plan view schematic layout of such a ring showing the various magnets, radio frequency power system and a 100 MeV electron linear accelerator injector. The four dipole magnets serve as the photon sources for the lithography stations.

Storage rings are injected with electrons from either microtrons or linear accelerators. Microtrons are small, but generally inject storage rings at a low rate compared to a linear accelerator. The location of the linear accelerator does not have to be on the same level as that of the storage ring so the injector system shown in figure 2 could be on a different floor. Besides electrical power, the only other service required by the storage ring is cooling water to remove the heat generated by synchrotron radiation, magnets and the radio frequency system. It should be noted that water pumps and power supply cooling fans are the only moving parts of such small simple storage rings. This accounts for their high reliability.

Table 1 lists a range of storage ring parameters. Of note here is the estimated half life of the electron beam. The electron beam in a storage ring decays due to electron-electron and electron-residual gas molecular collisions. To allow for a relatively constant wafer throughput it is envisioned that the ring would operate at a ring current that does not vary greatly, for example 600 to 400 mA. This means that injections would be required every 3-4 hours. From the experience of other small storage rings the total injection time is estimated to be around 5-10 minutes which represents a down time of less than 5% when

functioning in a continuous operational mode.

Figure 3 shows the variation in the orthogonal electron beam sizes (σ_x, σ_y) around the ring. The storage ring lattice allows some degree of flexibility of the source size but the source size would be in the region of 1.0 - 1.5 mm full width at half maximum (FWHM) in both vertical and horizontal dimensions for the electron beam within the dipole magnets. By considering slightly different electron optical lattices, the beam size could be decreased or increased if this was found to be necessary. The radiation is tightly collimated in the vertical plane with a vertical opening angle for 130 Å radiation of approximately ±1.0 mrads FWHM.

This then defines a simple and compact synchrotron storage ring of circumference = 16m that can be used as the basis of a light source for the collection optics.

5. Collection Optics for Synchrotron Radiation

Ideal condenser optics are required to gather a large percentage (or all) of the radiation emitted by the source, and condition this radiation in divergence, uniformity and direction to properly illuminate the mask and the imaging optics. An additional requirement of the condenser is to reduce the thermal load on the multilayer reflection mask. This can be achieved by having at least one of the optics in the illumination train coated with multilayers to monochromatize the white light from the synchrotron.

There are two types of mask geometries in lithography - rectangular fields as used in step and repeat cameras, and thin arc shaped fields as used in ring field scanning cameras. At present, the primary interest in SXPL is in scanning cameras of the type described by Jewell et al (9). This paper describes a four mirror ring field scanning camera that has a reduction ratio of 4:1, a mask object shape specified as an arc of radius 125mm, a chord length of 100mm and a ring width of 2mm. The direction of scan is to be in the width direction. Other parameters defining this camera are the pupil diameter (180mm) and the pupil to mask distance (3644mm) (16). This represents a possible prototype camera that would be built for a lithographic printer.

For this typical camera the mask numerical aperture (NA_{mask}) is about 0.025 where the numerical aperture is defined as the sine of the half angle subtended by the entrance pupil when viewed from a point on the mask. In lithography the sharpest high contrast images of small features are obtained when the radiation illuminating the mask does not completely fill the entrance pupil. The degree of coherency (σ) is defined as the fraction of the diameter of the pupil that is illuminated. A half filled pupil has $\sigma=0.5$. The task of the illuminator is to direct light through every part of the mask in a direction that passes through the pupil, half filling it (for $\sigma=0.5$). Thus every point on the mask should be illuminated with light of divergence $\Phi_{mask}=2\sigma NA_{mask}$ which is about 25 milliradians. Figure 4 shows a schematic diagram of how two points on an arc shaped mask need to be illuminated. Each point on the mask is illuminated with a cone of light with a full cone angle equal to $2\sigma NA_{mask}$, and directed at the center of the camera pupil. The center of the pupil is thus the

base of a multiplicity of light cones each with their apex at different points on the mask.

We know from simple ray optics that there exists an invariant, $I = S_o\Phi_o = S_i\Phi_i$, where S_o and S_i are respectively the object and image sizes and Φ_o and Φ_i are the angular divergences of the object and the image. Simply stated, when you magnify, the light becomes more collimated. This is a strong constraint. From above we have typically for the mask in the vertical direction I^v_{mask} = 2mm x 0.025rad = 0.05mm· rad and in the horizontal direction I^h_{mask} = 100mm x 0.025rad = 2.5mm· rad. For the storage ring we have, I^v_{synch} = 1mm x 0.002rad = 0.002mm· rad and in the horizontal, I^h_{synch} = 1mm x 1.0rad = 1.0mm· rad. In both cases the invariant (often called the LaGrange or the optical invariant) of the storage ring is smaller than that required for illuminating the mask. This is fortunate, because in an optical train, starting at the synchrotron and ending at the mask, it is always possible to increase the invariants by non-imaging optics, such as diffusers, flys' eye lenses, beam splitters, etc. It is not easy to decrease these invariants. The use of such non-imaging optics form the basis for a range of different illumination optic schemes that are best described by the following examples.

6. Illuminator Design 1 - Use of Scatter Plates

Figure 5 shows a schematic plan view of an illumination collection optical system. In the horizontal plane, mirror M1 collects about 500 mrads of light and directs it at a toroidal or ellipsoidal mirror M2. Mirror M2 focusses the light through the mask to form a focus at the center of the camera pupil. M2 is also required to shape the beam into the arc shape that is necessary to illuminate the reflection mask. Mirror M3 located between M2 and the mask is a scatter plate consisting of a mirror with a rippled sinusoidal surface (see figure 6). Light reflecting from M3 has its divergence increased such that the light then fills the camera entrance pupil to the required σ in the horizontal plane. The pupil filling factor is thus determined by the sinusoidal profile of the M3 scatter plate. This scatter plate is essentially a low period grating, and could be fabricated using existing grating technology. The grating pitch is large compared to the wavelength of the light used, so consequently there will be no detrimental diffraction effects. In the vertical plane, the light is tightly collimated from the storage ring. The vertical divergence of the light is also increased by the scatter plate M3, this time with a sinusoidal rippled surface perpendicular to the rippled surface scattering the radiation in the horizontal plane. Mirror M3 thus has a dimpled surface, the detailed shape of which determines how the pupil is filled.

The above illuminator description of figure 5 is a concept. Putting numbers into the concept allows one to see the practicality of such an illuminator scheme. The detailed discussion of the optical arrangement follows.

Synchrotron sources are unique optical light sources. The source is not located at a fixed point in space, but rather consists of different points on an arc as the electron beam moves in the bending magnet field. The light source is an incoherent continuum of sources each emitting a well collimated beam in the forward direction. Normally in x-ray optics a

toroidal or an ellipsoidal mirror would be used to collect and focus the radiation. Such an optical arrangement approximates the source as a single point, which is reasonable for small acceptance angles of synchrotron radiation (<30 mrads). For the collection optic mirror M1 that is required to collect 500 mrads and larger, such an approximation of the source as a single point is no longer valid. A mirror shape has been described by Lopez-Delgado and Szwarc (17) (LDS) that in principle allows collection and focussing of all 2π radians of light from a storage ring. Figure 7 shows two examples of the mirror shape, one for grazing incidence and the other for more normal incidence. This LDS mirror can collect the radiation from the distributed synchrotron source and focus it to a point. The mirror equation is given by (17) -

$$x = R\cos\alpha - \frac{0.5\,(d^2 - R^2 - a^2) + aR\sin\alpha}{d - a\cos\alpha}\sin\alpha$$

$$y = R\sin\alpha + \frac{0.5\,(d^2 - R^2 - a^2) + aR\sin\alpha}{d - a\cos\alpha}\cos\alpha$$

where x and y are the mirror coordinates in the orbit plane, R is the radius of the electron orbit, d is the total photon path length which is constrained to be fixed, a is the focus point along the Y axis and α is the angle subtended by the source about the X axis. Such a mirror is not a simple shape and would require a numerical mirror shaping machine for its fabrication. From figure 7 it is apparent that the grazing incidence LDS mirror is required to be longer than the normal incidence case when collecting the same horizontal fan of radiation. For this reason we opt for a normal incident LDS mirror for the schematic illuminator layout shown in figure 8.

The LDS mirror M1 collects 500 mrads of light and focusses the source in the horizontal plane with approximately 2:1 magnification to a point that acts as the source for the toroidal mirror M2. This arrangement allows the positioning of the camera away from the storage ring. M1 will be a difficult mirror to make as it a long mirror ($\sim$1500mm) and has light incident on it with a range of angles which require it to be coated with a graded multilayer mirror. The heat load that the mirror has to tolerate is only moderate being about 300 watts distributed along its 1500mm length with a vertical profile, defined by the opening angle from the storage ring, of about 2mm on the mirror. This corresponds to $\sim$10watts/cm^2, which is well within the typical mirror power loads that are presently used on synchrotron beamlines. Rather than have M1 create a virtual source for M2 as shown in Fig 5, a real source is preferred as a phosphor screen can be positioned at this focus point for diagnostic purposes.

The magnified elevation view in figure 8 shows a closer view of the mirrors M2 and M3 along with the 4 mirror camera (9). The toroidal mirror M2 is located 500mm from the source created by M1 and focusses the light in both the horizontal and vertical planes into the center of the camera pupil located 4000mm distant from M2, and 3644mm beyond the

reflection mask. Ray tracing indicates that M2 can be a simple toroid rather than a more complicated ellipsoid shape. This is due to the small source size created by M1, whereby the source points lie close to the optic axis and allow reasonable focussing with a simple toric shape. Light is incident on M2 at a grazing angle of 20° and with sagittal and meridional radii of 1450mm and 333mm respectively, the light falls on the reflection mask with the correct arc shaped curvature. The scatter plate M3 behaves as a plane mirror to invert the arc shape from M2 such that the arc is the correct orientation for the camera.

The width of the ring illumination on the mask is required to be 2mm. This requires there to be some vertical focussing of the radiation from the storage ring because with no vertical focussing the width of the light on the mask would be about 10mm and 80% of the light then wasted. The vertical collection efficiency can be improved by having a slight vertical curvature in mirror M1, and focussing the light in the vertical to the same point that the light is focussed in the horizontal. Light at this focus location will have a vertical size of about 2mm and a total vertical divergence of about 1 mrad (from the source magnification). The sagittal radii of mirror M2 reduces the vertical size a small amount before the light falls on the mask. Without mirror M3 the light would be about 2mm wide on the mask. Mirror M3 acts as a scatter plate adding divergence to the beam. In order not to increase the width of the light falling on the mask much beyond the 2mm, M3 has to be positioned close to the mask. A distance of about 75mm is reasonable whilst still maintaining space for the light to be reflected from the mask into the camera. The surface profile of M3 shown in figure 6 for one direction and is modulated as $(h/2)\sin(2\pi x/P)$, where h is the ripple height, x is the distance along the mirror and P is the period. The maximum slope is $\pm h\pi/P$. The incident light needs to be reflected into ±12.5mrads, requiring the maximum slope to be ±6.2mrads as the mirror reflects at twice the angle. For a period $P=200\mu m$ the ripple height is required to be 0.6μm. By making M3 with ripples in orthogonal directions the mirror is able to scatter the light in both directions and fill the pupil to the required σ. The orthogonal scattering of the light fills the pupil with a square shaped patch of light rather than the round patch shown in fig.4. This is not considered to have a great effect on the imaging characteristics of the camera. For some lithographic processes such as when using phase shifting masks it is sometimes desirable to change σ (18). For the illumination system described this would require changing the scatter plate M3. For σ equal to zero, M3 would be a plane mirror.

Illumination uniformity on the mask is a significant issue in lithography, and although the synchrotron is a uniform source, there may well be some slight non uniformities in the reflection efficiency of parts of the mirrors in the illumination train. For a scanning camera this is only important along the long length of the arc of light that illuminates the mask. Variations in light intensity along this arc can be adjusted for by trimming the width of this arc just before the reflection mask.

The throughput efficiency of the illumination arrangement described above is about 25%, being the product of the reflection from a multilayer mirror M1 (~50% reflectivity) and two grazing incident reflections from mirrors M2 and M3, which if coated with Rhodium would each have a reflectivity of ~70% at the 20° grazing angle used (19).

7. Illuminator Design 2 - Multifaceted Mirrors

The previous illumination scheme required the fabrication of the large and complicated shaped mirror M1 of fig.8. As an alternative, the collection of the initial large angle of radiation can be achieved using a multifaceted mirror. Figure 9 shows a schematic plan view of an illumination scheme in which, in the horizontal plane, M1' is a multiple array of small plane mirrors which direct the light through an aperture S1. This aperture is the source for an ellipsoidal mirror M2' which images S1 through the mask into the pupil of the camera (P1). The distances between S1, M2' and P1 are such that the magnified image of S1 in the pupil fills the pupil to the required σ value in the horizontal plane. M2' is also required to shape the beam into the arc shape required to illuminate the mask. In the vertical plane the light diverges from the storage ring until reflected from the vertically reflecting multifaceted mirror Mv, which redirects the light in the vertical plane such that the light converges to pass through the 2mm wide arc on the mask and then diverges to fill the pupil to the required σ value in the vertical plane. This is shown schematically in figure 10.

The above concept will be elaborated on with a more detailed description for the mirror locations and their dimensions.

The layout and dimensions of the mirrors is driven by the constraints of the camera. In fig.9, the mask can be viewed as being illuminated in the horizontal plane by a multiplicity of sources from along the stripe of illumination on the surface of mirror M2'. Each point on the mirror M2' has light reflecting from it with a range of angles $\Phi 2$ which overlap on the mask with the effect that every point on the mask has light reflecting from it with a range of angles Φm, directed at, and half filling the camera entrance pupil. Φm is defined by the camera as $2\sigma NA = 25$mrads. We have the geometric relation $\Phi 2 = \Phi m \cdot D5/(D4+D5)$. D5 is defined by the camera to be 3644mm and a reasonable value for D4 is 500mm to move the mirror away from the mask. This defines $\Phi 2 = 22$mrads. All the points along the mask must see a full range of angles of illumination, and thus there must be some excess illumination beyond the ends of the illuminated mask length Lm as shown in fig.9. The horizontal illuminated length (Lm2) of mirror M2' is set by the geometric relation $Lm2=Lm \cdot ((D5+D4)/D5)+(2 \cdot D4 \cdot \Phi m)$, where Lm is the chord length of the arc illuminating the mask as set by the camera to be 100mm. This defines Lm2 = 139mm. Other reasonable values for some of the dimensions are D1=1000mm, D2=5000mm and S1=25mm. The distance D3 is constrained to be $D3=S1/\Phi 2=1136$mm. This in turn determines $\Theta 2=Lm2/D3=0.12$ radians. Continuing to work backwards we have $Lm1=\Theta 2 \cdot D2=600$mm, which is the horizontal width of the collection mirror as seen by the mask. A point on the mask looking back towards the source will see a projected horizontal section of the mirror M1' that is $\Phi m \cdot (D2+D3+D4)$ long, which is 166mm in this example. Each facet on mirror M1' appears when looking backwards from the mask to have a horizontal width $Wm1=S1 \cdot D1/(D1+D2)=4.2$mm wide. Thus each point on the mask is illuminated by $|Lm1/Wm1| = |166/4.2| = 39$ points of radiation which is sufficient for the condenser to act as if it were a continuous distribution of radiation. The total number of

facets that make up mirror M1' is thus | 600/4.2 | =142 facets. Any more than this and the light would not be captured by the mask.

In the vertical plane the facetted mirror Mv is located at a distance D1+Dv1 from the source. The vertical height of the beam at Mv is therefore (D1+Dv1)· Φv mm, where Φv is the vertical opening angle of the radiation which is ±1mrad. To fill the pupil to the required σ value the beam height on mirror Mv is also required to equal Dv2· Φm mm. We also have Dv1+Dv2=D2+D3+D4. This defines Dv1=6035mm and Dv2=601mm.

Figure 11 shows a scale schematic plan view of the condenser described above. The length of the facetted collection mirror M1' is the result of projecting the distance Lm1 onto a circle of radius 1743mm, which results in D1=1000mm for an electron orbit radius of 1429mm. For the layout shown in figure 11 the length of mirror M1' is 1061mm, the width of each facet is 7.5mm and the mirror collects 0.6 radians. Each facet is required to be adjustable and is located close to the electron beam within the dipole vacuum vessel. The facets of M1' reflect the beam upwards with a 10° reflection, and direct the light through the aperture S1. Beyond S1 is the facetted mirror Mv located 7035mm distant from the source. Mirror Mv reflects the beam downwards through about 135 degrees onto mirror M2'. This arrangement requires Mv to be a multilayer coated facetted mirror. The vertical beam height at mirror Mv is approximately 14mm, and this is required to be reduced to at most 2mm at the mask. Mirror Mv could consist of 10 facets each 1.4mm in width that would create a 'focus' on the mask of with 1.4mm with some penumbral blurring on each side. The mask would thus be illuminated in the vertical with 10 points of illumination. This is somewhat less than the 39 illumination points in the horizontal plane, but in scanning the mask through the imaging field, there will be an adequate amount of averaging. The mirror M2' is required to be ellipsoid as the apparent source for this mirror is rather large with substantial off axis imaging requirements. Raytracing indicates that a suitable ellipsoid shape would have an eccentricity of 0.96, a directrix of 2718mm and a grazing angle of 20 degrees. With this ellipsoidal shape and the various distances, the mask is illuminated with approximately the correct arc shape of illumination. The throughput efficiency of this second illuminator arrangement is approximately 32% which is a little higher than the earlier illuminator example due to the smaller grazing angle on mirror M1'.

8. Other Condenser Systems, Capillary Array Condenser.

The two examples described above show that it is possible to devise illumination schemes that will allow illumination of the mask with the required amount of power. They represent a family of condensers that reduce the inherent high brightness of electron storage rings to match that of the requirements of the soft x-ray cameras. The exact details of any particular layout are heavily dependant on the camera used, but the general principles described can be used with different permutations of the optical elements used.

Other classes of optical elements could be considered as being able to supply the requirements of condensers. Kumakhov (20) has described the use of bundles of hollow

glass tubes, the internal walls of which are able to reflect x-rays with reasonable efficiency by virtue of the small internal grazing angle. These hollow glass tubes behave similarly for X-rays as fibre optics behave for visible light. Thus, such a bundle of hollow tubes could collect any amount of synchrotron radiation and direct it over the required area of the mask with the required range of angles and direction. Another variable that is available when using hollow tubes is to taper the diameter of the end of the tube. In this way the divergence of the light emerging form the tube can be increased (21). The efficiency of such hollow glass tubes have not been measured at soft x-ray wavelengths, but in view of the small grazing angles used it might be expected to have a throughput of around 50%.

Another variation of the multiple tube array has been described by Wilkins et al (22). In this paper the focussing and redirecting properties of microchannel plates when used with x-rays are described. This represents yet another optical element that could be used in a soft x-ray condenser system.

9. Proposed Floor Plan of a Storage Ring Source in a SXPL factory.

As an example of a floor plan for a SXPL factory, Fig.13 shows the plan view of a small 600 MeV storage ring supplying flux to 6 lithography cameras, which use about half of the available radiation. Beamlines 1-5 are the facetted mirror design and beamline 6 is the scatter plate design. With further design optimization the number of beamlines could be increased to about 8 or 10 before space restrictions apply. The injection system is not shown as it is on another level so as not to interfere with the beamlines. The overall floor plan measures about 15m x 20m of which only the lithography stations at the end of the beamlines need be in a clean room environment. It is estimated that the ring and injector described in section 4 would cost between $5-10M, of which about a quarter is for the injector system. This cost would be reduced after the initial parameters for the ring have been established and sources made on a more production style basis. It should be noted that if a SXPL facility requires more than one storage ring, additional injectors are unnecessary as the same injector can easily supply electrons to several storage rings.

10. Summary.

A first pass design study has been carried out for condenser systems that use a compact 600 MeV electron storage ring as a soft x-ray source for SXPL cameras. Two condenser designs were detailed, and the layout indicated that fabrication is within the feasibility of existing technology. A compact 600 MeV storage ring has been described which when coupled with large ($\Theta \geq$ 500mrad) condensers is capable of delivering in excess of 1 watt of 130Å light in a 2% bandpass with no debris problems. This is nearly an order of magnitude more power than required (128 mwatts) to yield a print rate of $1 cm^2/sec$ using the anticipated 5 mJ/cm^2 resists and the 60% reflectivity multilayer mirrors. The storage ring, which uses conventional electromagnets, is based upon highly reliable existing technology. Nothing fundamental in the condenser designs appears to prevent collection of larger angles up to and beyond a radian. This would allow for higher wafer throughput at print rates

greater than 1cm^2/sec.

Acknowledgement

The authors wish to thank J.B.Hastings for directing our attention to the interesting results of reference 17.

References

1. H.Kinoshita, K.Kurihara, Y.Ishii, and Y.Torii, "Soft x-ray reduction lithography using multilayer mirrors", J.Vac.Sci.Technol. **B7**, 1648-1651, (1989).

2. J.E.Bjorkholm, J.Bokor, L.Eichner, R.R.Freeman, J.Gregus, T.E.Jewell, W.M.Mansfield, A.A. MacDowell, E.L.Raab, W.T.Silfvast, L.H.Szeto, D.M.Tennant, W.K.Waskiewicz, D.L.White, D.L.Windt and O.R.Wood II, "Reduction imaging using multilayer coated optics: Printing of features of smaller than 0.1 microns", J.Vac.Sci.Technol. **B8**, 1509-1513, (1990).

3. D.A.Tichenor, G.D.Kubiak, M.E.Malinowski, R.H.Stulen, S.J.Haney, K.W.Berger, L.A.Brown, R.R.Freeman, W.M.Mansfield, O.R.Wood II, D.M.Tennant, J.E.Bjorkholm, A.A.MacDowell, J Bokor, T.E.Jewell, D.L.White, D.L.Windt, and W.K.Waskiewicz, "Diffraction limited soft x-ray projection imaging using a laser plasma source", Opt.Let. **16**, 1557-1559, (1991).

4. D.J.Nagel "Plasma sources for x-ray lithography", VLSI Electronics, Vol 8, (New York : Academic Press, 1984).

5. P.Gohil, H.Kapor, D.Ma, M.C.Peckerer, P.J.MacIlrath and M.L.Ginter, "Soft x-ray lithography using radiation from laser produced plasmas", App.Opt. **24**, 2024-2027, (1985).

6. J.B.Murphy, "X-ray lithography sources: A review", Proc. 1989, IEEE Part.Acc.Conf. 757-760, (1989).

7. R.Heese, "Status of the National Synchrotron Light Source", Proc. 1987 IEEE Part.Acc.Conf. 400-404, (1987).

8. D.L.White, J.E.Bjorkholm, J.Bokor, L.Eichner, R.R.Freeman, J.Gregus, T.E.Jewell, W.M.Mansfield, A.A. MacDowell, E.L.Raab, W.T.Silfvast, L.H.Szeto, D.M.Tennant, W.K.Waskiewicz, D.L.Windt and O.R.Wood II, "Soft x-ray projection lithography : experiments and practical printers", SPIE, X-ray/EUV Optics for Astronomy, Microscopy, Polarimetry and Projection Lithography, Vol. 1343, 204-216, (1990).

9. T.E.Jewell, K.P.Thompson, J.M.Rodgers, "Reflective Optical Designs for Soft X-Ray Projection Lithography" SPIE Proc. Vol 1527, 163-173, (1991).

10. K.Kurihara, H.Kinoshita, T.Mizota, T.Haga and Y.Tori, "Two mirror telecentric optics for soft x-ray reduction lithography", J.Vac.Sci.Technol. **B9**, 3189-3192, (1991).

11. D. L. Windt, R. Hull, and W. K. Waskiewicz,"Interface imperfections in Metal/Si multilayers", J. Appl. Phys., **71**, 2675-2678, (1992).

12. D.M.Tennant, A.A.MacDowell, P.P.Mulgrew, J.Z.Pastalan, W.K.Waskiewicz, D.L.Windt

and O.R.Wood II, "Mask technologies for soft x-ray projection lithography at 13nm", This conference, 1992.

13. A.A.MacDowell, J.E.Bjorkholm, J.Bokor, L.Eichner, R.R.Freeman, W.M.Mansfield, J.Pastalan, W.T.Silfvast, L.H.Szeto, D.M.Tennant, W.K.Waskiewicz, D.L.White, D.L.Windt, O.R.Wood II and F.Zernike, "Soft x-ray projection lithography using a 1:1 ring field optical system", J.Vac.Sci.Technol. **B9**, 3193-3197, (1991).

14. J.B.Kortright and J.H.Underwood, "Design considerations for multilayer schwarzschild objective for the XUV", SPIE vol 1343 95-103 (1990).

15. G.K.Green, "Spectra and Optics of synchrotron radiation", BNL Report 50522, (1976).

16. T.E.Jewell, private communication.

17. R.Lopez-Delgado and H.Szwarc, "Focussing of All the synchrotron radiation (2π radians) from an electron storage ring on a single point without time distortion", Optics Comm. **19**, 286-291, (1976).

18. D.W.Johnson and C.A.Mack, "Modelling the continuing realm of optical lithography" Semicond. Int. **15**, 134-140 (1992)

19. D.L.Windt, W.C.Cash, M.Scott, P.Arendt, B.Newnam, R.F.Fisher and A.B.Swartzlander,"Optical constants for thin films of Ti, Zr, Nb, Mo, Ru, Rh, Pd, Ag, Hf, Ta, W, Re, Ir, Os, Pt and Au from 24Å to 1216Å", App.Opt. **27**, 246-278, (1988).

20. M.A.Kumakhov, "Channeling of Photons and new X-Ray Optics", Nucl. Instrum. Meth. **B48**, 283-286, (1990).

21. D.J.Thiel, D.H.Bilderback, A.Lewis, E.A.Stern and T.Rich, "Guiding and concentrating hard x-rays by using a flexible hollow core tapered glass fiber", App.Opt. **31**, 987-992, (1992).

22. S.W.Wilkins, A.W.Stevenson, K.A.Nugent, H.Chapman and S.Steenstrup, "On the concentration, focussing, and collimation of x-rays and neutrons using microchannel plates and configurations of holes", Rev.Sci.Instrum. **60**, 1026-1039, (1989).

Figure Captions

1. Plot of the dipole power output of storage rings versus photon wavelength for different electron energies. The magnetic field of the dipole magnet is fixed at 1.4 Tesla.

2. Plan layout of a proposed 600 MeV storage ring with the 100 MeV linear accelerator electron injector system. The four items labelled 'D' are the dipole magnets that are the soft x-ray light sources.

3. Plot of beam size versus distance around the circumference of the storage ring. The items labelled 'D' are the dipole magnets. Only half of the ring is shown as it has a center of symmetry.

4. Schematic view of 2 points on a mask illuminated with an arc shaped patch such that all the light at each point of the illuminated part of the mask passes through the center part of the camera entrance pupil. For the schematic view here the mask is treated as a transmission mask.

5. Schematic plan view of a condenser system using scatter plates.

6. Schematic view of a one dimensional scatter plate of period P and ripple height h.

7. Two layouts of the LDS mirror. The circles represent the electron orbit that is emitting synchrotron radiation. a) shows the case for a normal incidence collection mirror, b) shows the case for a grazing incidence collection mirror,

8. Schematic scale plan and elevation views of the condenser utilizing a normal incidence LDS mirror M1, a toroid M2, and a scatter plate M3. The mask, wafer and the 4 mirror camera (9) are also shown in the expanded inset of the elevation view.

9. Schematic plan view of a condenser system using multifaceted mirrors.

10. Schematic elevation view of the multifaceted mirror Mv that redirects the light in the vertical plane through the 2mm wide mask illuminated region and into the pupil with the correct angular spread for the pupil fill factor σ. For the schematic view here the mask is treated as a transmission mask.

11. Schematic scale plan and elevation views of the condenser system using multifaceted mirrors M1' and Mv. Mirror M2' is an ellipsoidal mirror. The mask, wafer and the 4 mirror camera (9) are also shown in the expanded inset of the elevation view.

12. Schematic plan view of the 600 MeV storage ring and 6 lithography cameras (numbered). The cameras are illuminated with light using the 2 condenser designs described in the text. The electron injection system is not shown as it is on another level so as not to interfere with

the beamlines.

Table Captions.

Table 1. Various parameters for the 600 MeV storage ring.

P(λ) [mW/0.5 amp/0.5 rad/2% BW] versus λ

E [MeV]	400	600	800
ρ [m]	0.95	1.43	1.91
B [T]	1.4	1.4	1.4
λ_c [Å]	83.2	37.0	20.8

E = 400 MeV
E = 600 MeV
E = 800 MeV

P(λ) [mW/0.5 amp/0.5 rad/2% BW]

0
2000
4000
6000
8000

0
50
100
150
200

λ [Å]

FIG 1

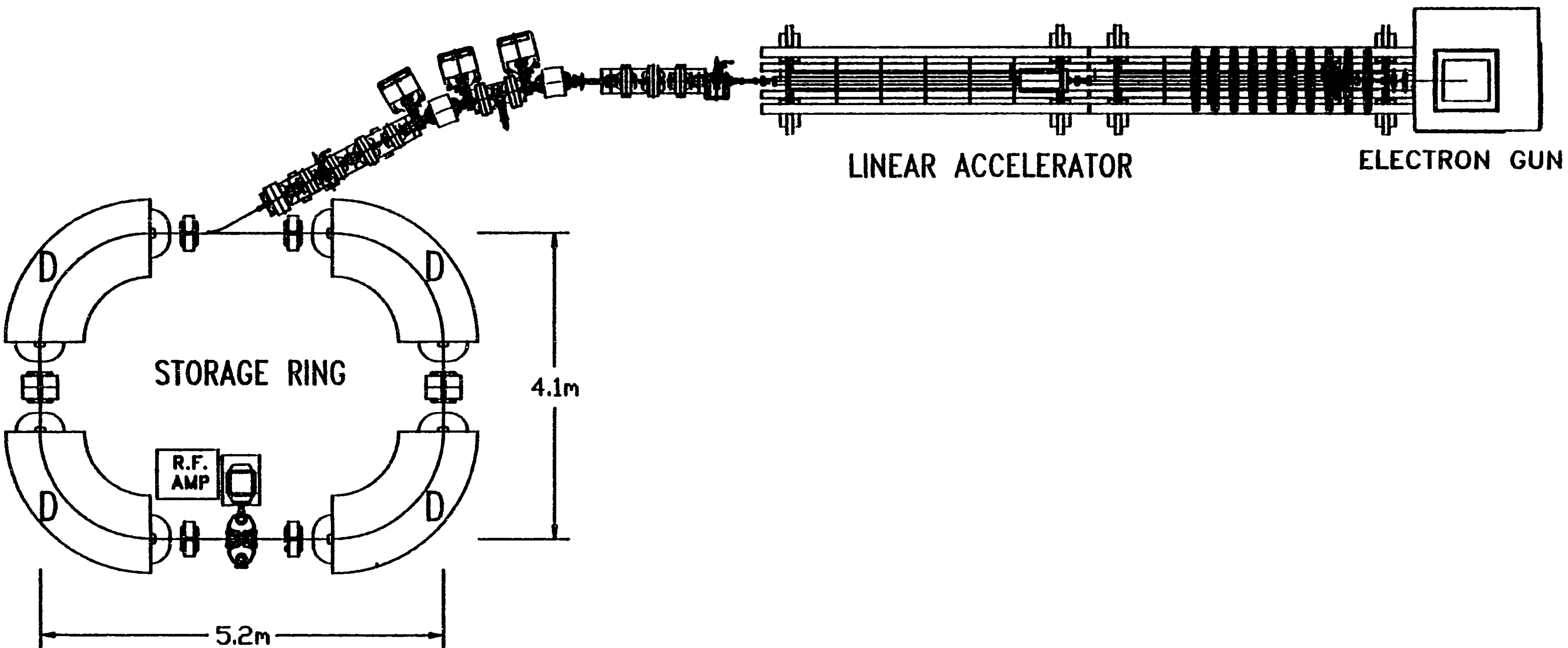

FIG.2

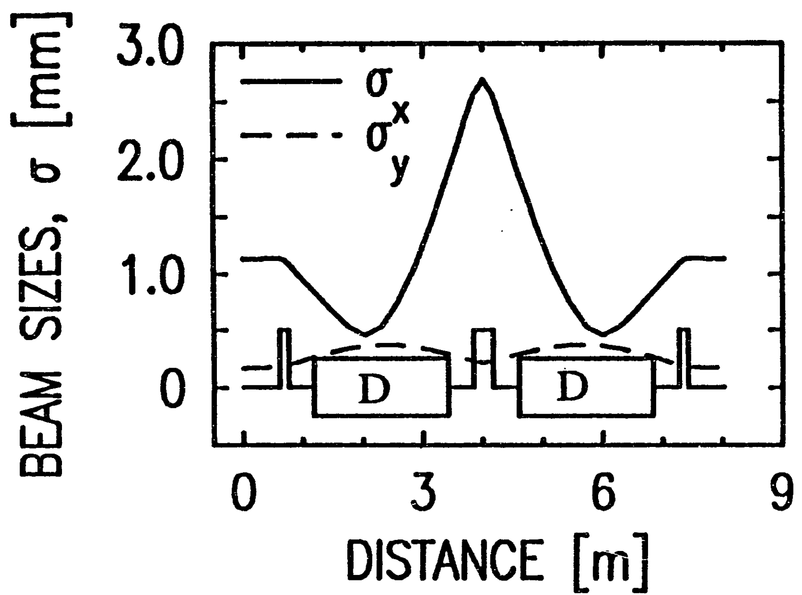

FIG. 3

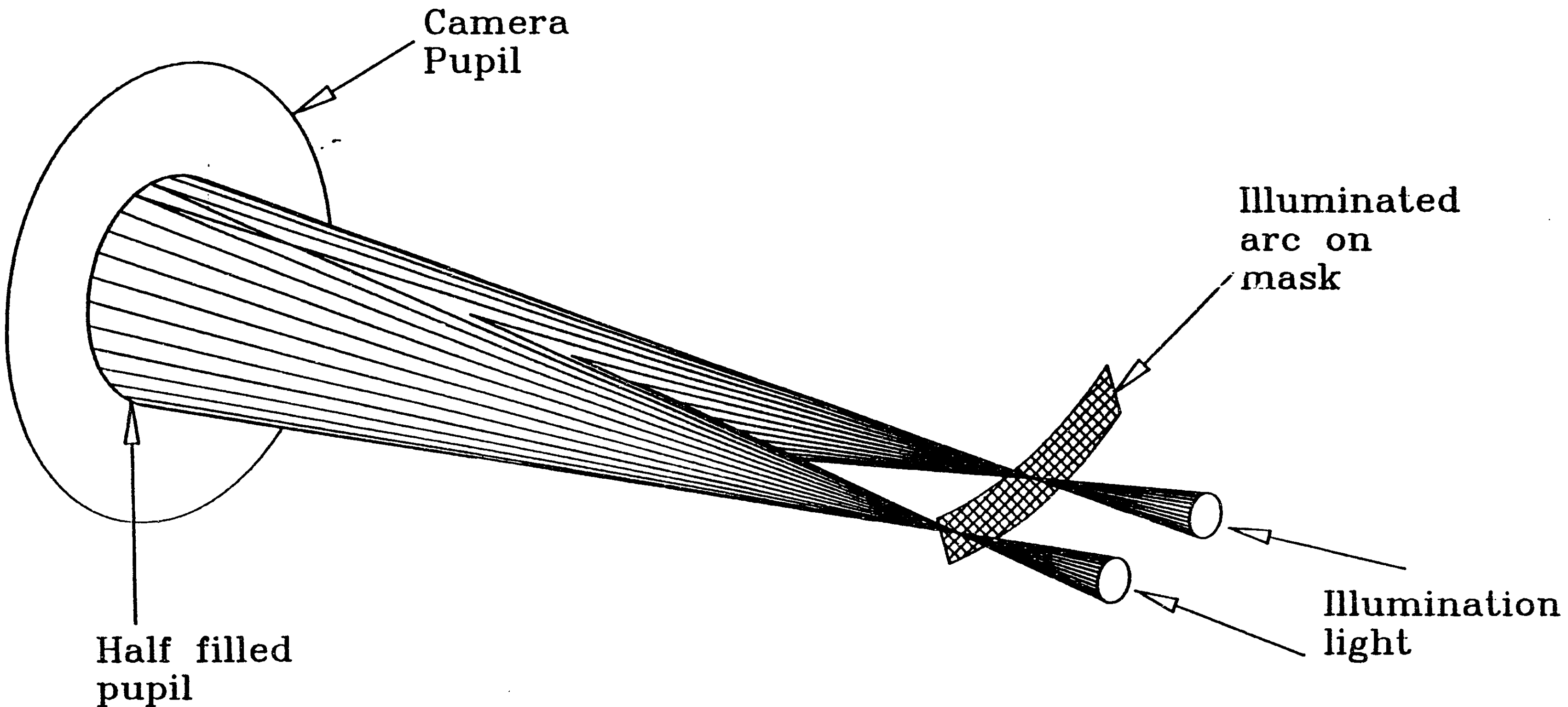

fig.4

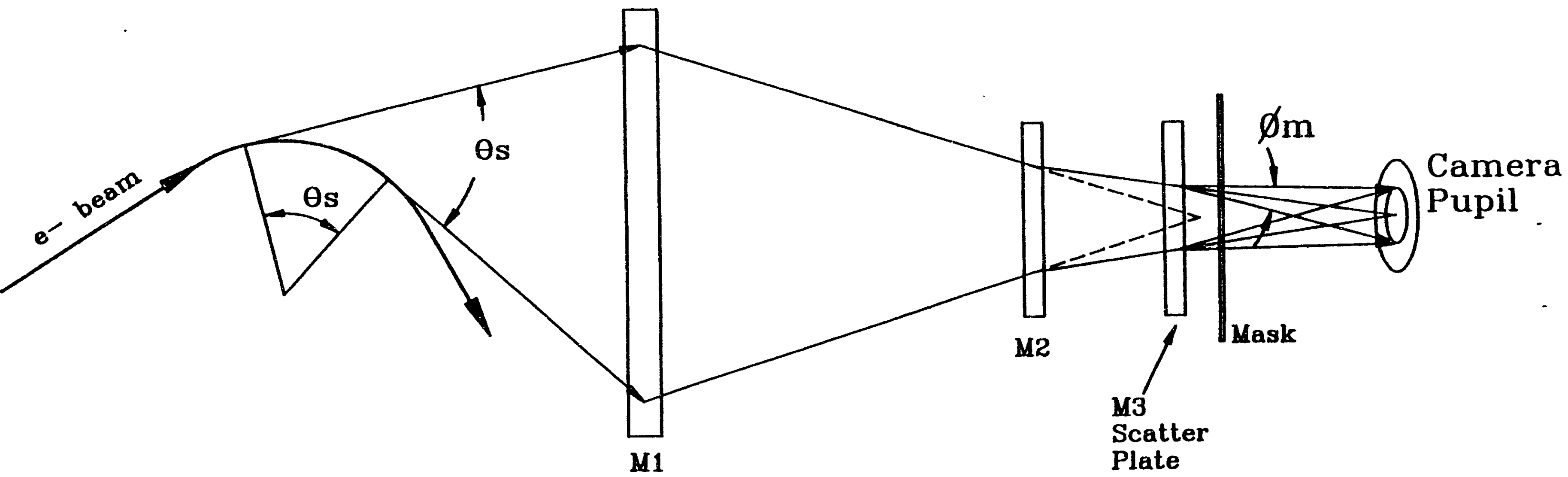

Fig.5

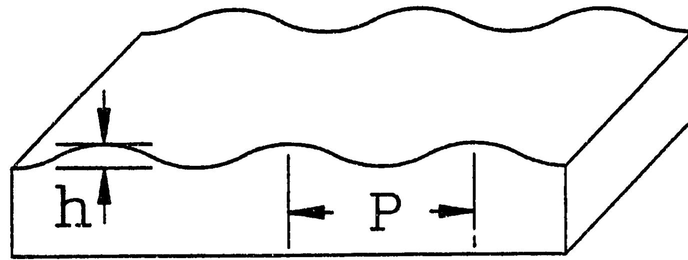

Fig. 6

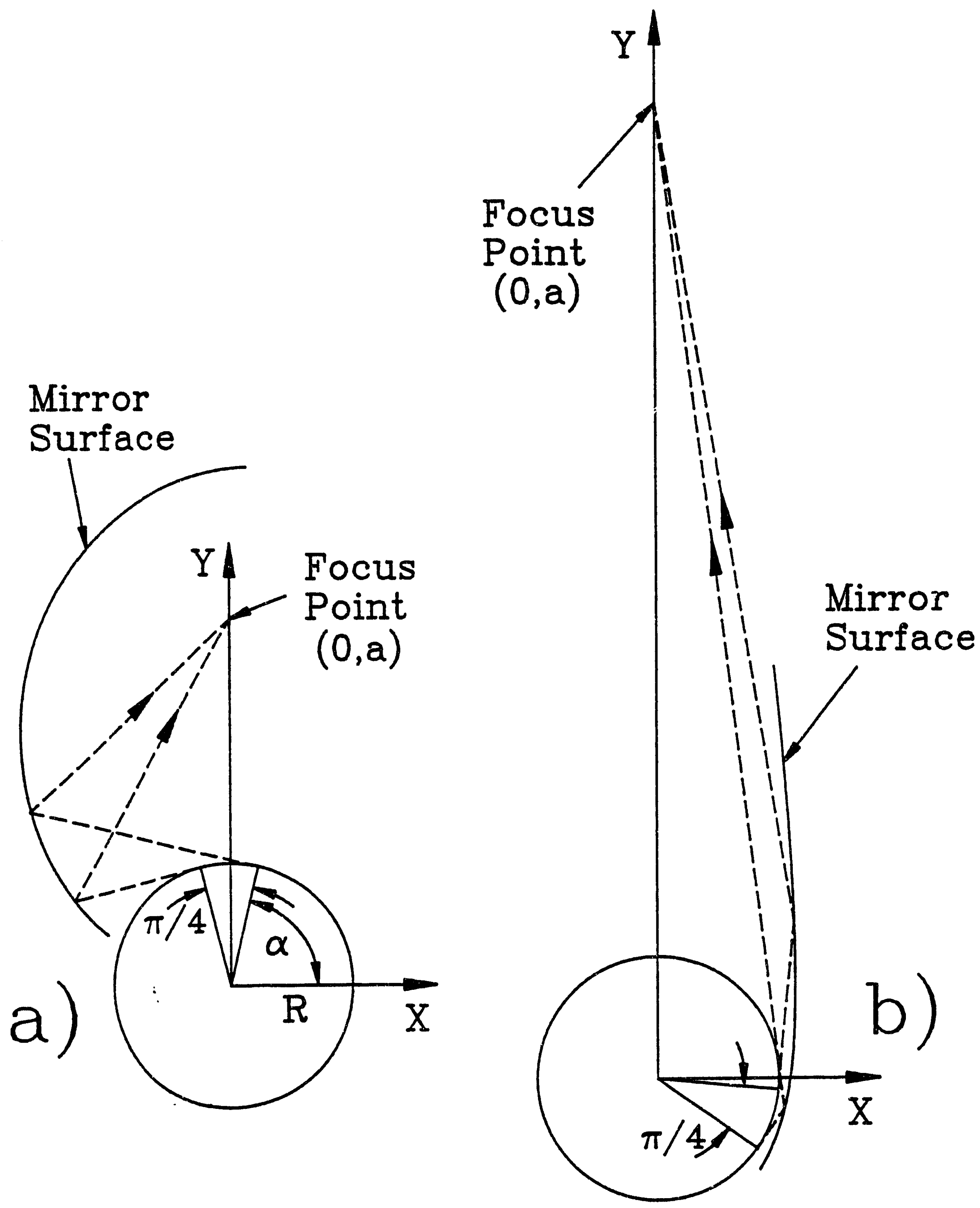

Fig 7

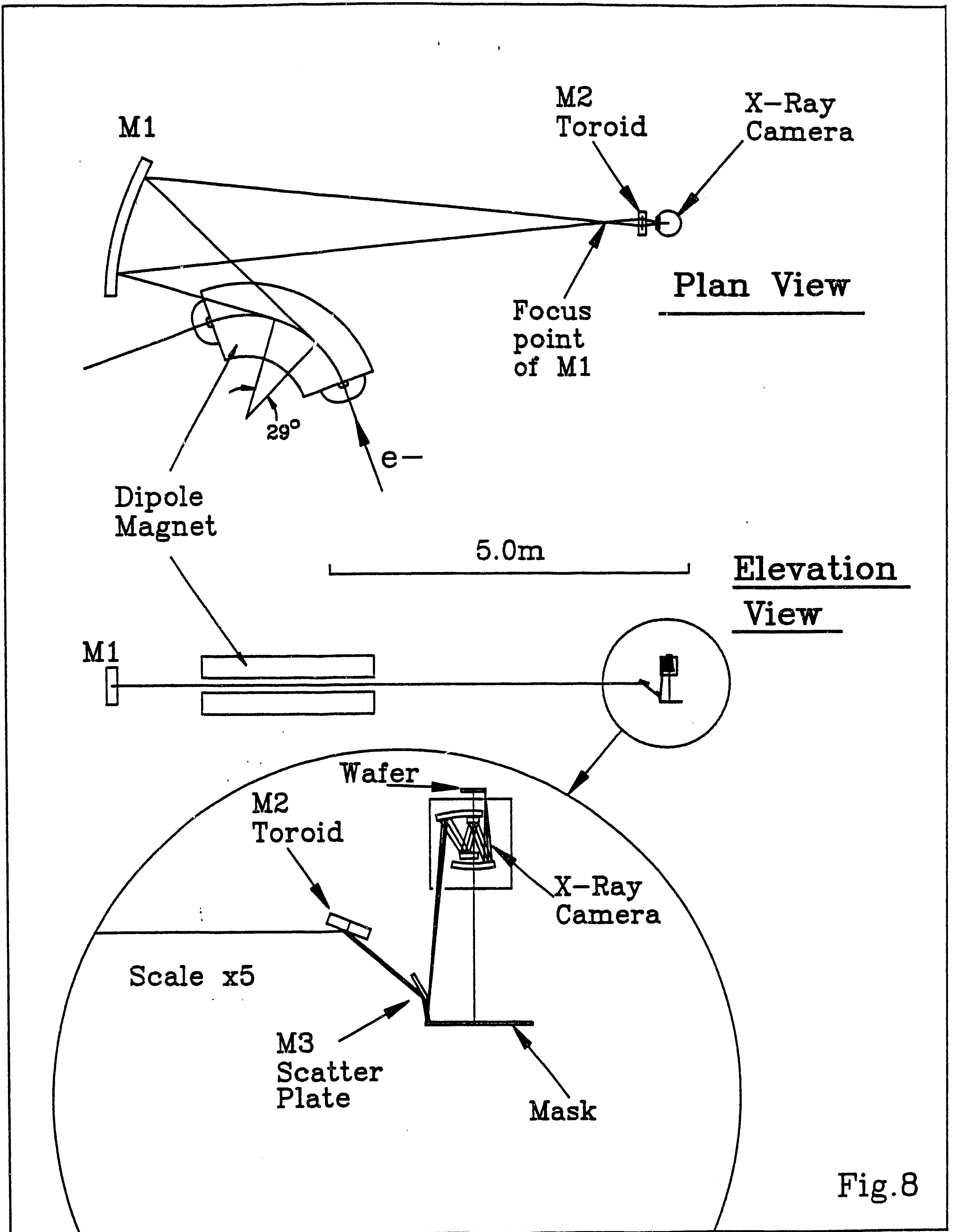

Fig.8

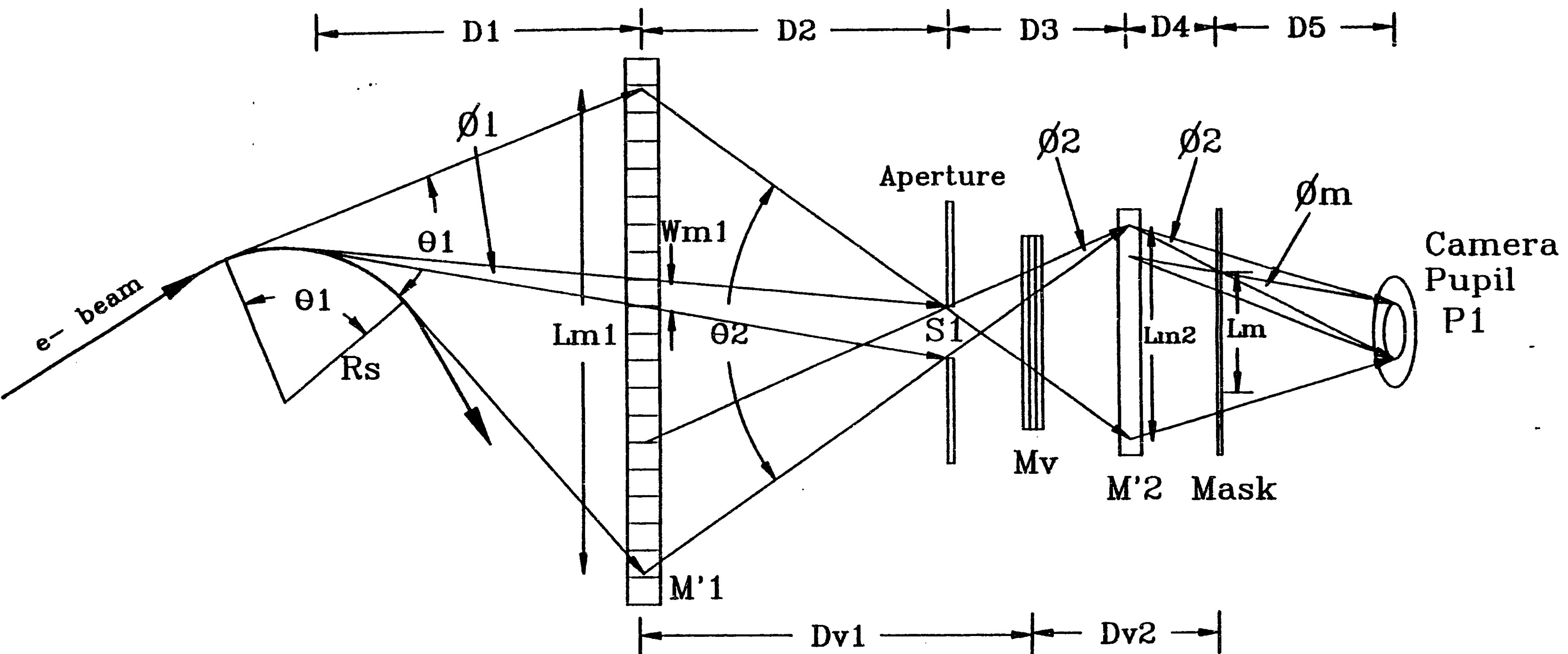

Fig.9

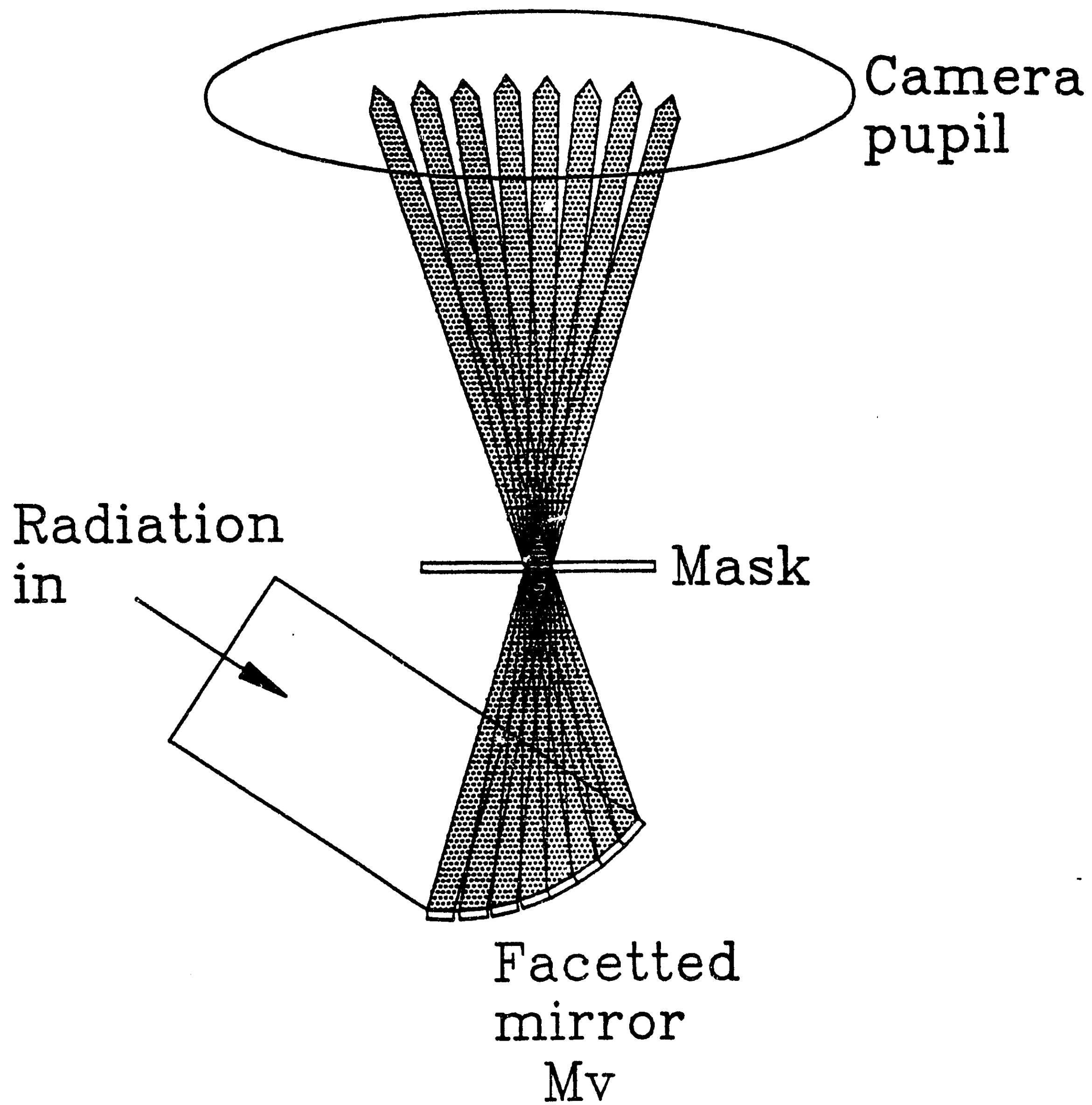

Fig 10

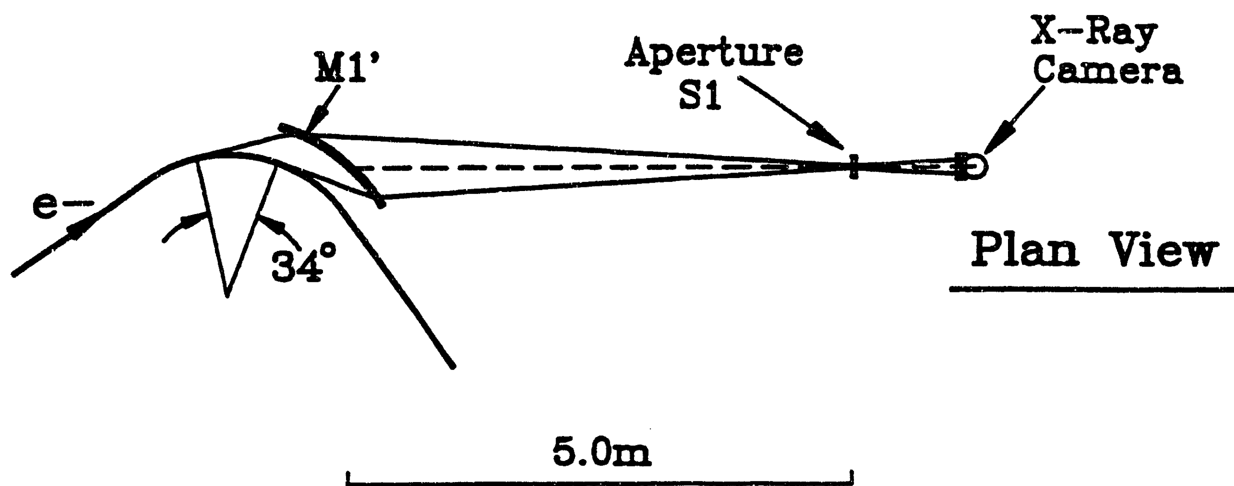

Dipole
Magnet
M1'
Elevation
View
Mv
Wafer
Scale x5
X-Ray
Camera
M2'
Ellipsoid
Aperture
S1
Mask

Fig.11

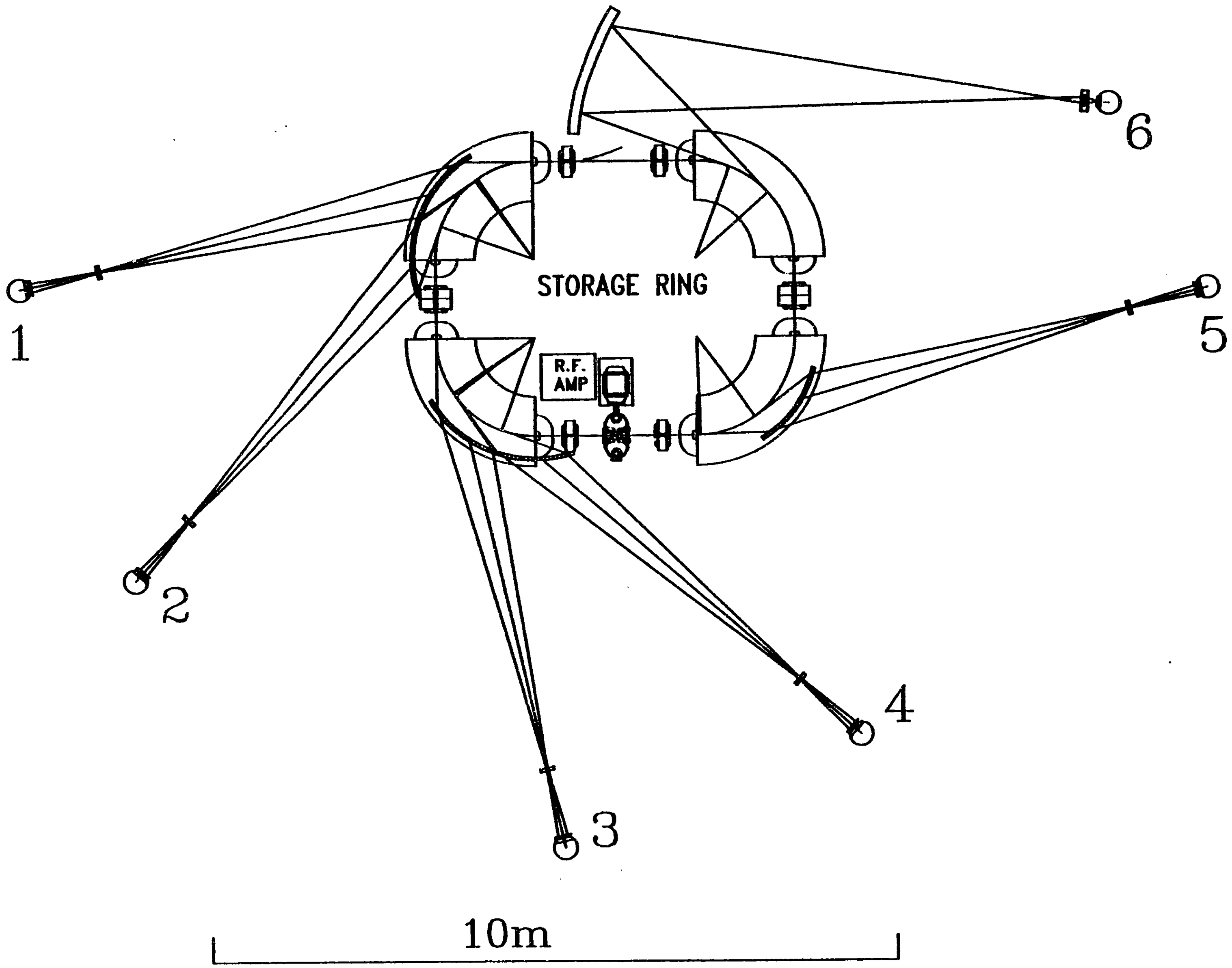

fig.12

Energy	600MeV
Circumference	16.0m
Type	DBA
Bending Radius ρ	1.429m
Dipole Field	1.4 Tesla
Emittance ε_0	2.0×10^{-7} m-rad
Total Radiated Power	4Kwatt/500mA/2πrad
Critical Wavelength	36.9 Å
Lifetime	3-4 hours

DISCLAIMER

This report was prepared as an account of work sponsored by an agency of the United States Government. Neither the United States Government nor any agency thereof, nor any of their employees, makes any warranty, express or implied, or assumes any legal liability or responsibility for the accuracy, completeness, or usefulness of any information, apparatus, product, or process disclosed, or represents that its use would not infringe privately owned rights. Reference herein to any specific commercial product, process, or service by trade name, trademark, manufacturer, or otherwise does not necessarily constitute or imply its endorsement, recommendation, or favoring by the United States Government or any agency thereof. The views and opinions of authors expressed herein do not necessarily state or reflect those of the United States Government or any agency thereof.

TABLE 1

END

DATE
FILMED
1 / 13 / 93